Sonoluminescence bubble measurements using vision-based algorithms

Nancy R. Hall[a], Jeffrey R. Mackey[b] and Thomas J. Matula[c]
[a]NASA John H. Glenn Research Center 21000 Brookpark Road, Cleveland, Ohio 44135
[b]MK Optics Inc., 10473 Misty Ridge, Concord, Ohio 44077
[c]Applied Physics Laboratory, University of Washington, 1013 NE 40th St., Seattle, WA 98105

ABSTRACT

Vision-based measurement methods were used to measure bubble sizes in this sonoluminescence experiment. Bubble imaging was accomplished by placing the bubble between a bright light source and a microscope-CCD camera system. A collimated light-emitting diode was operated in a pulsed mode with an adjustable time delay with respect to the piezo-electric transducer drive signal. The light-emitting diode produced a bubble shadowgraph consisting of a multiple exposure made by numerous light pulses imaged onto a charge-couple device camera. Each image was transferred from the camera to a computer-controlled machine vision system via a frame grabber. The frame grabber was equipped with on-board memory to accommodate sequential image buffering while images were transferred to the host processor and analyzed. This configuration allowed the host computer to perform diameter measurements, centroid position measurements and shape estimation in "real-time" as the next image was being acquired. Bubble size measurement accuracy with an uncertainty of 3 microns was achieved using standard lenses and machine vision algorithms. Bubble centroid position accuracy was also within the 3 micron tolerance of the vision system. This uncertainty estimation accounted for the optical spatial resolution, digitization errors and the edge detection algorithm accuracy. The vision algorithms include camera calibration, thresholding, edge detection, edge position determination, distance between two edges computations and centroid position computations.

Keywords: Sonoluminescence, bubble, machine vision, algorithms, centroid position,

1. INTRODUCTION

Sonoluminescence (SL) is the emission of light from a bubble undergoing radial oscillations. In single bubble SL, a micron-sized bubble is levitated against buoyancy forces by a sound pressure produced in the water-filled containment vessel by transducers. The position of the bubble is determined by the position of this antinode, which is governed largely by the containment vessel geometry. The acoustic standing waves (sinusoidal waves) force the bubble into radial pulsations. During tensile-pressure cycles, the bubble expands (approximately ten-fold); after which the pressure changes sign, driving the bubble into a violent inertial collapse. A pulse of ultraviolet and visible light is produced at the end of the collapse.

Single bubble SL was first observed in 1989 by graduate student D. Felipe Gaitan[1] at the University of Mississippi. Prior to that time, research in the area of SL involved unstable single bubbles, or fields of bubbles being created and destroyed.[2] The discovery of single bubble SL made it possible for researchers to concentrate on the behavior of a single bubble as opposed to the cloud of bubbles as in multibubble SL. However, it wasn't until Seth Putterman's group at UCLA repeated Gaitan's experiment and started publishing some of their results[3,4] that other researchers started to take notice. As interest in SL grew, many questions resulted from these early experiments such as how does one determine the bubble's radius[5], does the bubble remain spherical throughout the acoustic cycle, and what is

[a] nancy.r.hall@grc.nasa.gov; phone 1 216 433 5643; fax 1 216 433 8050
[b] jeff.mackey@mkoptics.com; phone 1 440 350 9966
[c] matula@apl.washington.edu; phone 1 206 685 7654

the bubble dynamics that is occurring during the SL process[6,7]. To gain some understanding of the bubble dynamics of a SL bubble, one must first understand what is happening to a bubble during the SL process.

Figure 1 illustrates the nonlinear response of a SL bubble to an applied sound field. At the start of the acoustic cycle, the bubble radius is estimated be on the order of 3-8μm. During the negative portion of the sound field, the bubble starts to expand. This is due to pressure inside the bubble falling below the vapor pressure of the liquid and the air bubble starts to fill with vapor. The bubble continues to expand, up to a radius of about 50 μm until the sound field turns positive. This, in turn, causes the bubble to implode with such a violent collapse that at the end of the collapse, it emits a pulse[8], on the order of 50-300 picoseconds of a bluish light which is in the ultraviolet and visible part of the spectrum. Following the collapse the bubble isn't extinguished, but actually rebounds. Then, this process is repeated during the next acoustic cycle. The temperature inside the bubble during the collapse is estimated to be on the order of thousands of degrees Kelvin[9,10,11] and pressures on the order of several kilobars.

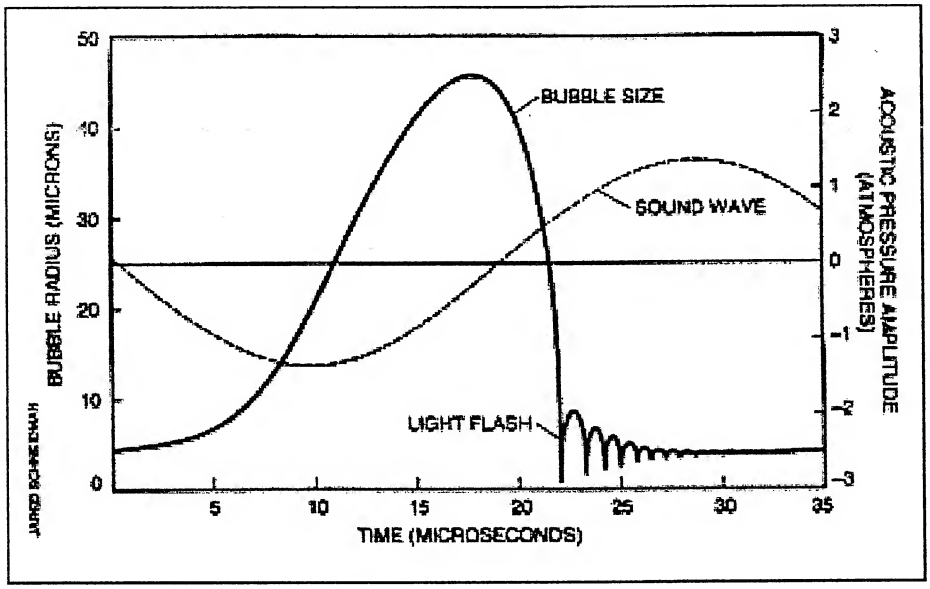

Figure 1: The growth and collapse of bubble's radius in response to a pressure amplitude of the driving sound wave versus time. This represents one acoustic cycle during the SL process. (Source: S.J. Putterman, Scientific American 272, 46, 1995)

While the sound field does play a role in the radial oscillations of the bubble, several other forces have an effect on the bubble's position and size. During SL, a bubble created through a rapid boiling process is levitated in an acoustic standing wave. This occurs when the Bjerknes force[12],

$$F_{Bjerknes} = -V(t)\nabla P_a \tag{1}$$

where V(t) is the instantaneous volume of the bubble and Pa is the forcing acoustic pressure, is balanced against the buoyancy force:

$$F_{buoyancy} = \rho g V(t) \tag{2}$$

The Bjerknes force will tend to force the bubble toward an acoustic pressure antinode whose position is governed largely by the containment vessel geometry. Also, the bubble is attracted to this antinode when the driving frequency is below its natural resonance frequency. However, as the magnitude of the forcing pressure changes, this has an

effect on both the degree of growth and the degree of collapse, which occur as the driving pressure increases on the bubble.

In order to understand single-bubble SL, it is important to measure the bubble oscillations during a given acoustic cycle, and to compare those measurements with expected behavior. In addition, it is of interest to look for Rayleigh-Taylor instabilities during the collapse and parametric instabilities during the rebounds[13]. In this paper, vision-based algorithms for making these measurements are discussed.

Since the gas bubble changes rapidly in size, it must be imaged at distinct temporal phases relative to the sound pressure field. Because the positional stability may be affected by small perturbations, it is necessary to quantify the amount of motion associated with the bubble as the sound pressure level is changed. A machine vision based imaging system is required to acquire and process bubble images under high-magnification in order to compute diameter measurements, shape estimations and centroid positions *in-situ*.

2. EXPERIMENT CONFIGURATION

The SL experiment configuration consisted of the following pieces of hardware: a square cross-sectional acrylic chamber, a nickel-chromium sparker wire, a high-frequency linear amplifier, 300mH inductor, an acoustic horn consisting of several piezo transducers stacked end-to-end, a sine wave generator and de-gassed water within the SL chamber. The water was de-gassed by boiling it, sealing the boiling vessel and then chilling it in ice water for a period of approximately five minutes. The experimental configuration used to collect the imaging data is shown in the Figure 2.

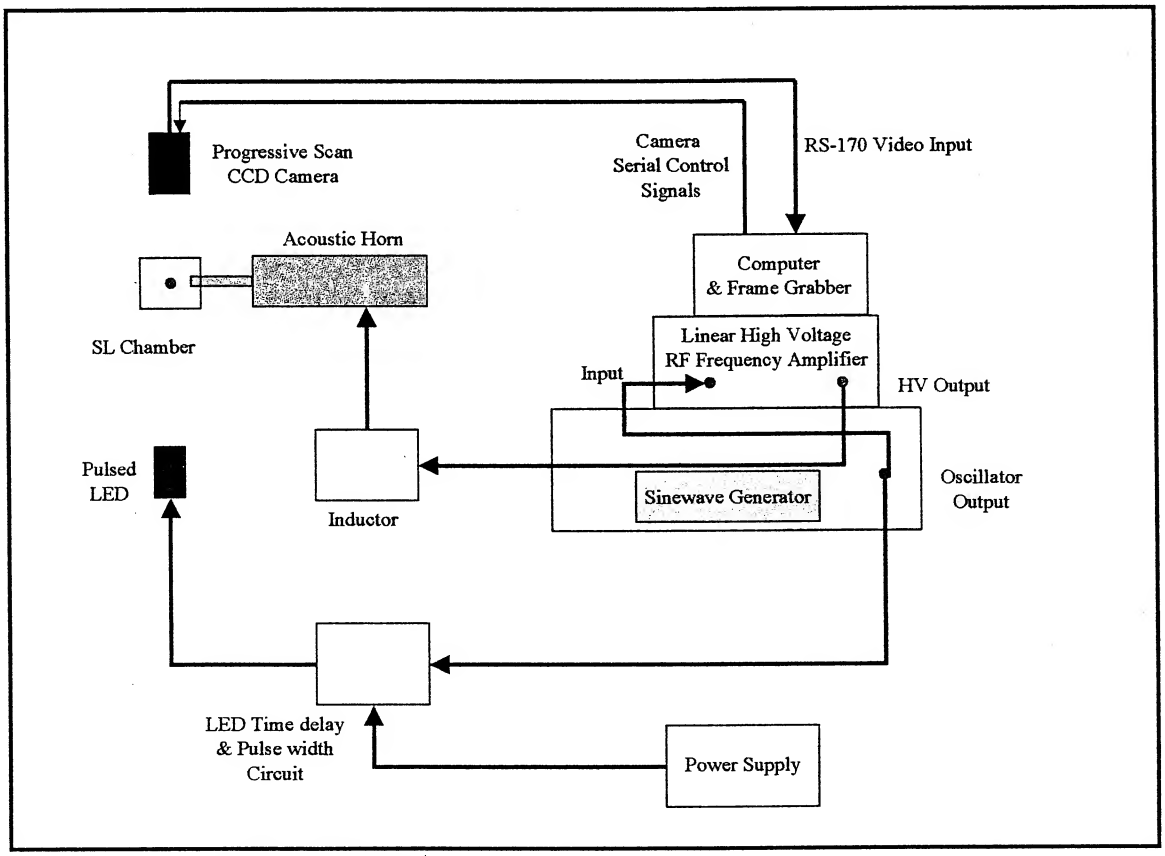

Figure 2: SL experiment configuration

It was necessary to image the SL bubble at its maximum radius (Rmax) as well as at its equilibrium radius (Ro), where Ro occurs at the position where the acoustic pressure amplitude crosses zero in the negative direction (Fig. 1). Therefore, the levitated sonoluminescing air bubble was imaged under a collimated pulsed LED backlight using a standard progressive scan CCD camera. A long working distance microscope (Infinity model K2) was used to provide adequate magnification in order to make the appropriate diameter measurements. The LED backlight was synchronized with the sound pressure wave (piezo-transducers in the acoustic horn) and images were grabbed and analyzed at a rate of 29.97 frames per second using a 1GHz computer and frame grabber. It is important to note that the CCD camera cannot keep pace with the SL backlight pulses. Therefore, since the camera exposure time was set to 33ms, each processed image is a time exposure of many stroboscopic images at the same point in the acoustic cycle. The imaging configuration used in the experiment is diagrammed in the Figure 3.

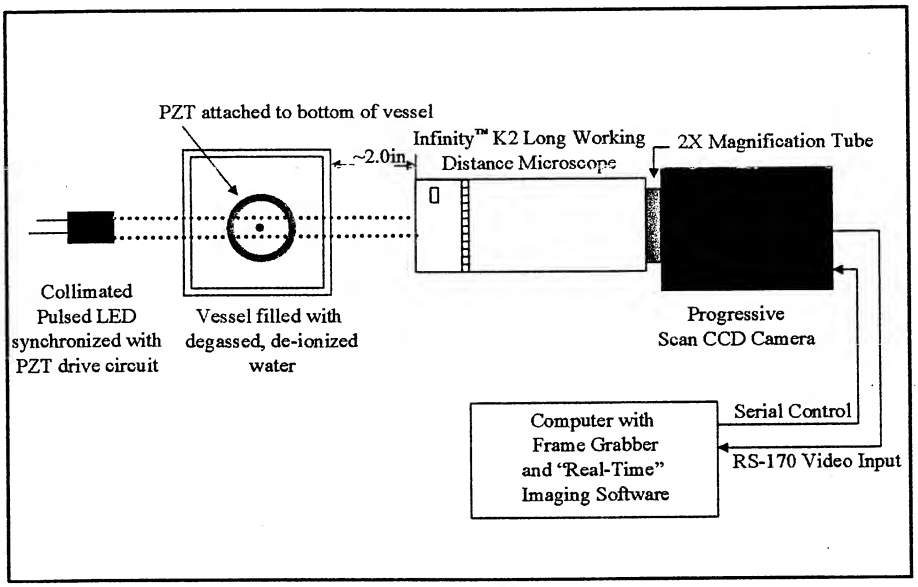

Figure 3: Imaging configuration for SL experiment

From the imaging system just described, a magnification of 20X was obtainable at appropriate working distances. This magnification was sufficient to provide useable image data for size analysis. Since the largest anticipated bubble diameter was approximately 120μm, that size would be imaged onto 2.4mm of the image plane.

3. RESULTS AND DISCUSSION

An overview of the interior of the SL chamber containing a levitated SL bubble is shown in Figure 4. A sense of size perspective regarding the bubble may be inferred from the photograph since the sparker wire probe is approximately 5mm in diameter.

In order to make a fairly accurate bubble diameter measurement, the camera must be calibrated. To accomplish this task, several custom chrome-on-glass targets were manufactured and provided by Applied Image Incorporated. The targets (Fig. 5) were made with 5μm diameter dots arranged in a repetitive square grid pattern.

These targets were tested using a calibrated microscope system at NASA Glenn Research Center and found to have a spacing of 312μm. Prior to imaging a SL bubble, one of these targets was placed at the midpoint in the SL chamber in order to provide a reference image for calibration purposes.

Images of the SL bubble were obtained at Ro and Rmax. These images were processed and analyzed to obtain diameter measurements at both sizes of interest. The image processing was optimized for speed, and therefore, employed a simple set of functions. The main step was to perform a connectivity analysis. In order to perform this processing step, the image must be binarized, and thus, a threshold operation had to be performed first. A gray level cutoff value of 73 was chosen and all pixel values greater than 73 were set to 255 (white) while all pixels having intensity values lower than 73 were set to 0 (black).

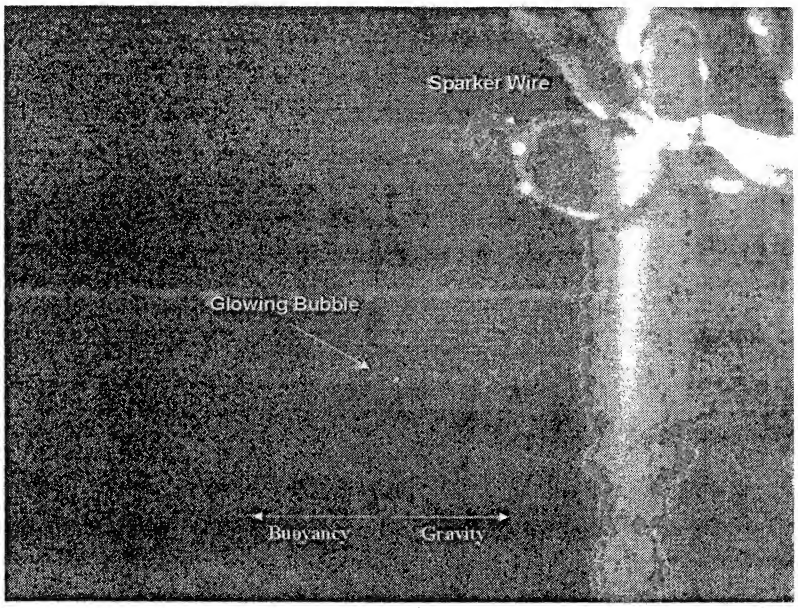

Figure 4. Overview of sonoluminescing bubble in cube-shaped vessel. The image was captured using a low magnification in order to show the sparker wire used to produce the air bubble.

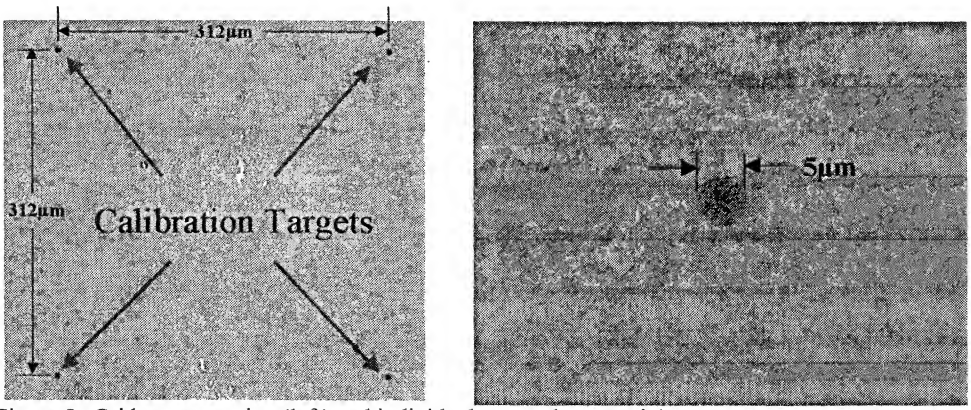

Figure 5. Grid target spacing (left) and individual target element (right).

The thresholding process provided a realistic representation of the edge position of the SL bubble. The diameter measurement could then be computed in pixel space based upon the edge coordinate profile. Since we were interested only in the horizontal and vertical diameter measurements, a connectivity[14] analysis was performed so that each set of connected pixels of grey level value zero could be bounded by a box having a length and width equal to the horizontal and vertical bubble diameters respectively. The original and processed images are shown in Figure 6.

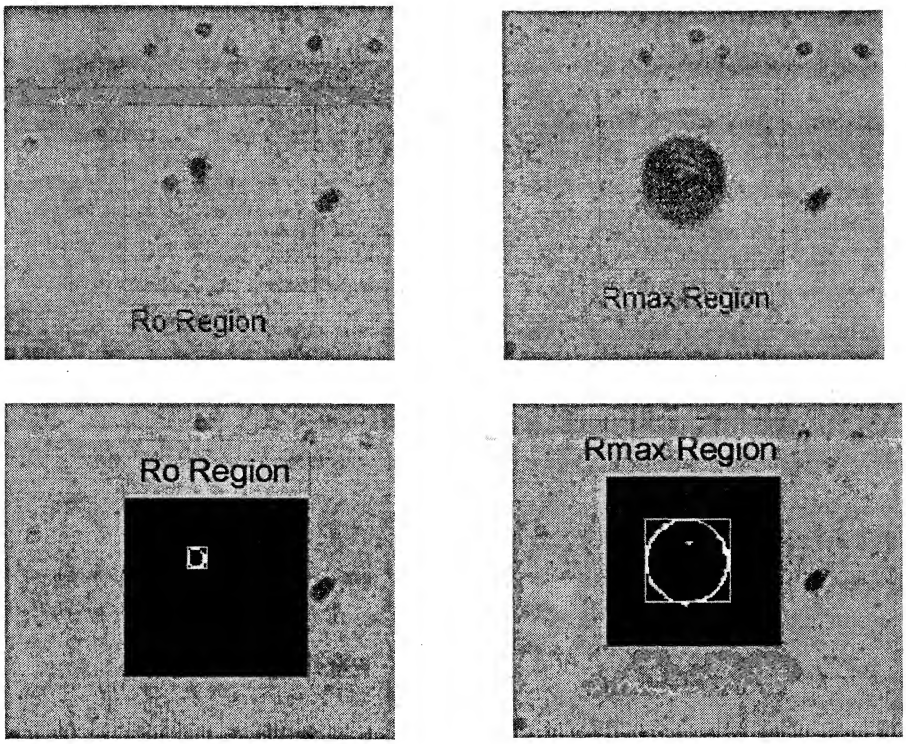

Figure 6. Original and processed bubble images showing Ro (top left), Rmax (top right), Ro bounded after being processed (bottom left) and Rmax bounded after being processed (bottom right).

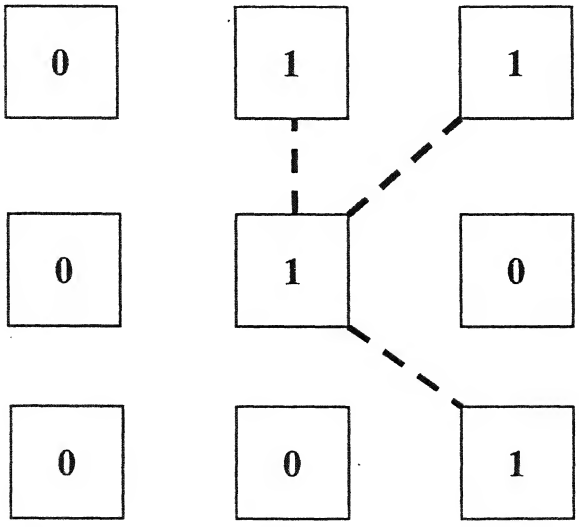

Figure 7. Diagram of 8-neighbors of the central pixel.

The connectivity analysis mathematically determines if two pixels are adjacent to each other. In the case of an object defined by its edges, such as the bubble under investigation, the algorithm must use 8-connectivity. This implies that two pixels r and s are 8-connected if s is in the set $N_8(r)$. The principle of 8-connectivity is illustrated in Figure 7.

If 4-connectivity were used instead of 8-connectivity, only the pixel directly above the central pixel would be located. In our image processing algorithms, we must use 8-connectivity since we are examining a curved surface where edges will likely be located on the diagonals.

Based on the processed images, the maximum diameter measurements were found to be 256 pixels vertically and 257 pixels horizontally. Applying the appropriate calibration factor, these pixel space values correspond to vertical and horizontal diameter measurements of 115.2μm and 115.7μm respectively. The equilibrium diameter measurements were 18 pixels vertically and 17 pixels horizontally, which corresponds to 8.1μm and 7.65μm respectively.

4. CONCLUSIONS AND FUTURE WORK

Based on the experimental data, it is possible to achieve Ro and Rmax diameter measurements to accuracy of approximately 3μm. Based on radius as a function of time SL plot (Fig. 1.), Ro and Rmax occur for several microseconds at SL frequencies, and therefore, the temporal resolution is more forgiving and does not greatly affect the spatial resolution of the diameter measurement. In the future, it would be of scientific value to get diameter measurements of a SL bubble at various points along the radius as a function of time SL plot to better observe the bubble as it expands and contracts. This should lead to a better understanding of the bubble dynamics of a SL bubble including its shape and size not only during its growth and its collapse, but also during the rebounds following light emission.

ACKNOWLEDGEMENTS

This work is supported by NASA NAG3-2379. NRH thanks John McQuillen of NASA GRC for answering many questions on various aspects of this research paper. JRM wishes to acknowledge Rick Rogers of NASA GRC for providing test images of calibration targets using his calibrated digital video microscope system. The authors also wish to acknowledge the NASA GRC BDiSL Team (Eric Bruckner, Dwayne Kiefer, Elizabeth Gray, Kirk Logsdon, Robert Skupinski, Jeremy Young) for their insightful work.

REFERENCES

1. D.F. Gaitan, *An Experimental Investigation of Acoustic Cavitation in Gaseous Liquids,* PhD Thesis, University of Mississippi, 1990,
2. M. P. Brenner, S. Hilgenfeldt, D. Lohse, "Single Bubble Sonoluminescence", *Review of Modern Physics*, **74**, pp. 425-484, 2002
3. S.J. Putterman, "Sonoluminescence: Sound into Light", *Scientific American*, pp. 32-37, 1995
4. R. A. Hiller and B.P. Barber, "Producing Light from a Bubble of Air", *Scientific American*, pp. 96-98, 1995
5. M. P. Brenner, S. Hilgenfeldt, D. Lohse, "Sonoluminescence: The hydrodynamical/chemical approach: A detailed comparison to experiment" in the NATO ASI Proceedings on the 1997 Leavenworth conference on Sonochemistry and Sonoluminescence, edited by L. Crum (Kluwer Academic Publishers, Dordrecht, 1997).

6. B.P. Barber, et al, "Defining the Unknowns of Sonoluminescence", *Physics Reports,* **281,** pp. 65-143, 1987
7. D.F. Gaitan, L.A. Crum, C.C. Church and R. A. Roy., "Sonoluminescence and bubble dynamics for a single, stable, cavitation bubble" *J. Acoust. Soc. Am.,* **91,** (6), pp. 3166-3183, 1992
8. T. J. Matula, Science Requirements Document, NAG3-2379
9. Hilgenfeldt, S., S. Grossmann, et al. "A simple explanation of light emission in sonoluminescence." *Nature* **398** (6726): pp. 402-405, 1999
10. Moss, W. C., D. A. Young, et al. "Computed optical emissions from a sonoluminescing bubble.", *Physical Review E* **59** (3): 2986-2992, 1999.
11. Hammer, D. and L. Frommhold,. "Sonoluminescence: how bubble glow," *Journal of modern optics,* **48** (2): pp. 239-277, 2001
12. L.A. Crum, "Bjerknes forces on bubbles in a stationary sound field", *J. Acoust. Soc. Am.* **57,** pp. 1363-1370, 1975
13. T.J. Matula, "Bubble Levitation and translation under single-bubble sonoluminescence conditions", *J. Acoust. Soc. Am* **114** (2) pp. 775-781, 2003.
14. R. C. Gonzolez and R. E. Woods, "Digital Image Processing", Addison-Wesley Publishing Company, Reading, MA, pp. 41-43, 1992.